
Improving the Spatial Alignment in PET/CT Using Amplitude-Based Respiration-Gated PET and Patient-Specific Breathing-Instructed CT

Charlotte S. van der Vos^{1,2}, Antoi P.W. Meeuwis¹, Willem Grootjans³, Lioe-Fee de Geus-Oei^{2,3}, and Eric P. Visser¹

¹Department of Radiology and Nuclear Medicine, Radboud University Medical Center, Nijmegen, The Netherlands; ²University of Twente, Enschede, The Netherlands; and ³Department of Radiology, Leiden University Medical Center, Leiden, The Netherlands

Appropriate attenuation correction is important for accurate quantification of SUVs in PET. Patient respiratory motion can introduce a spatial mismatch between respiration-gated PET and CT, reducing quantitative accuracy. In this study, the effect of a patient-specific breathing-instructed CT protocol on the spatial alignment between CT and amplitude-based optimal respiration-gated PET images was investigated. **Methods:** ¹⁸F-FDG PET/CT imaging was performed on 20 patients. In addition to the standard low-dose free-breathing CT, breath-hold CT was performed. The amplitude limits of the respiration-gated PET were used to instruct patients to hold their breath during CT acquisition at a similar amplitude level. Spatial mismatch was quantified using the position differences between the lung–liver transition in PET and CT images, the distance between PET and CT lesions' centroids, and the amount of overlap as indicated by the Jaccard similarity coefficient. Furthermore, the effect on attenuation correction was quantified by measuring SUVs, metabolic tumor volume, and total lesion glycolysis (TLG) of lung lesions. **Results:** All patients found the breathing instructions feasible; however, 4 patients had trouble complying with the instructions. In total, 18 patients were included. The average distance between the lung–liver transition between PET and CT was significantly reduced for breath-hold CT (1.7 ± 2.1 mm), compared with standard CT (5.6 ± 7.3 mm) ($P = 0.049$). Furthermore, the mean distance between the lesions' centroids on PET and CT was significantly smaller for breath-hold CT (3.6 ± 2.0 mm) than for standard CT (5.5 ± 6.5 mm) ($P = 0.040$). Quantification of lung lesion SUV was significantly affected, with a higher SUV_{mean} when breath-hold CT (6.3 ± 3.9 g/cm³) was used for image reconstruction than for standard CT (6.1 ± 3.8 g/cm³) ($P = 0.044$). Though metabolic tumor volume was not significantly different, TLG reached statistical significance. **Conclusion:** Optimal respiration-gated PET in combination with patient-specific breathing-instructed CT results in an improved alignment between PET and CT images and shows an increased SUV_{mean} and TLG. Even though the effects are small, a more accurate SUV and TLG determination is of importance for a more stable PET quantification, which is relevant for radiotherapy planning and therapy response monitoring.

Received Jun. 18, 2018; revision accepted Oct. 9, 2018.
For correspondence or reprints contact: Charlotte van der Vos, Department of Radiology and Nuclear Medicine, Radboud University Medical Center, P.O. Box 9101, 6500 HB Nijmegen, The Netherlands.
E-mail: charlotte.vandervos@radboudumc.nl
Published online Nov. 9, 2018.
COPYRIGHT © 2019 by the Society of Nuclear Medicine and Molecular Imaging.

Key Words: amplitude-based optimal respiratory gating; lung tumors; image quantification in PET; spatial alignment; breath-hold CT

J Nucl Med Technol 2019; 47:154–159
DOI: 10.2967/jnmt.118.215970

Since the introduction of hybrid PET/CT imaging, there have been attempts to improve the alignment between PET and CT images (1–4). Appropriate spatial matching is of importance for accurate anatomic localization of radio-tracer uptake, essential for adequate diagnosis and staging of a disease (2,5). Besides visual interpretation, CT scans are used for attenuation correction of the PET data (1,2,6,7), where a mismatch can result in quantitative inaccuracies (8). This can be particularly problematic for lesions near structures with large differences in density, such as lung lesions. Accurate image quantification is the first step to using PET for personalizing medicine, providing the ability to more adequately plan therapy and monitor treatment response (2,9–11).

Particularly in thoracic and abdominal PET/CT imaging, issues regarding spatial overlap between the 2 image-sets arise because of respiratory motion. Respiratory motion in PET results in quantitative inaccuracies due to the blurred appearance of moving structures, which needs to be corrected (1,6,7,10,12). A CT acquisition takes only several seconds and can therefore already be considered a respiratory motion-free image (1,6,7). However, combining the respiration-gated PET and the CT images is not always easy. Respiratory gating protocols result in a PET image at a certain time point during the respiratory cycle, and this time point does not necessarily correspond to the phase in which the CT image was captured. Therefore, respiratory gating could further reduce the spatial alignment between PET and CT images, resulting in an under- or overestimation of the SUVs (3,6,7,10,13).

Even though breathing-instructed CT protocols are the most straightforward approach to improving spatial alignment between respiration-gated PET and CT images, the use of simple instructions can be difficult to implement for

operators and patients and can have variable results. Some studies reported a clear improvement when breathing instructions were used (8,13), whereas other studies did not show an improvement (or yielded even worse results) (14). To overcome these discrepancies between simple breathing instructions and to gain more control over the exact respiratory amplitude at which the CT is acquired, the use of a patient-specific breath-hold CT protocol is proposed in this study. In this protocol, the respiratory signal is used both for the reconstruction of the amplitude-based respiration-gated PET images and for the patient-specific breathing instructions during the CT acquisition.

MATERIALS AND METHODS

Testing of the Protocol

Before the start of the study, 5 patients were asked to perform 2 types of breathing instructions to check the feasibility of the acquisition protocol. These 5 patients received a standard PET/CT scan. For the first type of breathing instruction, patients were asked to breathe normally until they were instructed to hold their breath for 10 s. For the second type of instruction, which was performed at least 1 min later, the patients were asked to take a couple of deep breaths, after which they were asked to hold their breath during the same expiratory phase and for the same duration of 10 s. For both types of instruction, the respiratory signal was measured and used to determine the specific moment of the breath-hold instruction given by the operator. All 5 patients could comply with both types of breathing instruction without any difficulty. The first instruction was chosen because it was easier for the operator to determine the exact moment that the respiratory signal reached the correct amplitude and because the breathing pattern of the patients was more comparable to the breathing pattern during the PET acquisition.

Patients

The local Institutional Review Board approved the protocol, and informed consent was obtained from all patients (including the patients who tested the breathing instructions). Twenty patients with suspected lung cancer were prospectively included in this study and received an ^{18}F -FDG PET/CT scan with an additional low-dose breath-hold CT scan. Patient characteristics are summarized in Table 1. The administration of ^{18}F -FDG was nonlinearly dependent on patient weight (15). The administered activity is given by

$$A = 0.036 \times m^2,$$

where A is the activity (MBq) and m the body mass (kg). The mean administered activity (and SD) was 210 ± 105 MBq, with a mean incubation time of 63 ± 6 min.

PET Acquisition and Respiratory Gating

A Biograph 40 mCT PET/CT scanner with an extended field of view (TrueV) was used (Siemens Healthcare). This scanner is accredited by the Research 4 Life initiative for quantitative PET/CT imaging (16). The PET images were acquired using an optimized, amplitude-based respiratory gating algorithm (HD•Chest) that was integrated in the PET/CT software. Respiratory gating was performed on bed positions covering the thorax and upper abdomen. Gated and nongated bed positions were acquired during free breathing for 6 and 2 min, respectively. Respiratory gating

TABLE 1
Patient Characteristics

Characteristic	Data
Sex (<i>n</i>)	
Male	12
Female	8
Mean age (y)	64.2 (SD, 9.2)
Mean weight (kg)	76.3 (SD, 18.1)
Mean administered activity (MBq)	210 (SD, 105)
Diagnosis (<i>n</i>)	
Primary lung cancer	10
Metastasis	6
Other and unconfirmed	4
Location of lesion (<i>n</i>)	
Upper lobes	16
Middle and lower lobes	9
Lung hilum	6

was performed with a duty cycle of 35%, providing a good balance between image quality and motion rejection (7). The longer acquisition time for the gated bed positions (thorax and upper abdomen) than for the nongated ones led to images with similar statistical quality after gating. The respiratory signal was acquired using a respiratory gating system with a pressure sensor integrated in an elastic belt placed around the patient's abdomen (AZ-733V Electronics; Anzai Medical Co, Ltd.).

PET Image Reconstruction

The PET images were reconstructed using 3-dimensional ordered-subset expectation maximization with a spatially varying point-spread function (TrueX) incorporating time-of-flight information (UltraHD PET). Image reconstruction was performed with 3 iterations and 21 subsets. The slice thickness of the PET images was matched to that of the attenuation CT images. Postreconstruction filtering was performed using a 3-dimensional gaussian filter kernel with a full width at half maximum of 3.0 mm. A transaxial matrix size of 400×400 (with a pixel size of 2×2 mm) was used for the PET reconstructions. All PET images were reconstructed using the respiration-gating algorithm.

Standard Low-Dose CT Protocol

A standard low-dose spiral CT scan was acquired with a free-breathing protocol. The x-ray tube voltage was chosen using CARE kV, with a reference tube voltage of 120 kV. The tube current was modulated using CARE Dose4D, with a reference tube current of 50 mAs. CT images were made with a 0.5-s rotation time, a pitch of 1, and 16×1.2 -mm collimation. A reconstruction with an increment of 3.0 mm and a reconstructed slice thickness of 5.0 mm was made for the attenuation correction. To quantify the lung–liver boundary and to delineate the lung lesions, the anatomic CT with a reconstructed slice thickness of 3.0 mm, a sharper reconstruction kernel, and a smaller field of view was used.

Patient-Specific Breathing–Instructed CT Protocol

During the additional low-dose spiral CT acquisition, the respiratory signal of the patient was measured and the PET amplitude range was used to provide specific breathing instructions for each patient. Before the start of the PET/CT scan, the breathing protocol was practiced to make sure that all patients understood the breathing instructions and could hold their breath for at least 10 s.

The tube voltage was chosen using CARE kV, with a reference tube voltage of 100 kV. The tube current was modulated using

CARE Dose4D, with a reference tube current of 35 mAs. These values were lower than the standard low-dose CT to reduce the radiation dose for the patient. Other acquisition and reconstruction settings were similar to the 2 reconstructions of the standard low-dose CT, except for the higher pitch (1.5 instead of 1) to reduce scan time for the breath-hold protocol.

Breathing Instructions

To analyze the effect of breathing instructions on the alignment between respiration-gated PET and CT, patients who did not perform the breathing instruction correctly were excluded from analysis. Correct execution of the breath-hold protocol by the patient was determined by measuring the average breathing amplitude before the start of the CT scan and during the CT acquisition. The ratio between the 2 amplitudes was calculated to determine whether the patient managed to comply with the instructions, which means that with a lower ratio less respiratory motion is present in the breath-hold CT image (Fig. 1 provides a visual explanation of the used amplitude ranges).

Image Analysis

The PET and CT images were analyzed using the Inveon Research Workplace software, version 4.1 (Siemens). Spatial alignment between anatomy on PET and CT was quantified using 4 methods. First, spatial mismatch was quantified by measuring the position differences for the liver dome in the craniocaudal direction. The liver dome was determined visually on the PET and CT images in the transaxial plane (using the lung setting for CT, window center: -450 Hounsfield units; width: 1,500 Hounsfield units). To quantify the alignment of the lung lesions, the lesions were delineated in the PET and CT images. In the PET images, lesions were delineated using a fixed-threshold region-growing segmentation algorithm. The segmentation threshold was set to 40% of the SUV_{max} , which is recognized as a suitable threshold for delineation of lung lesions (17,18). The lesions in the CT images were manually delineated using the lung setting. In the second method, the alignment of the lesions was determined by

quantifying the distance between PET and CT lesions' centroids, and in the third method, the spatial overlap between the lesions on PET and CT was determined using the Jaccard similarity coefficient, defined as

$$J(\text{VOI}_{CT}, \text{VOI}_{PET}) = \frac{\text{VOI}_{CT} \cap \text{VOI}_{PET}}{\text{VOI}_{CT} \cup \text{VOI}_{PET}}$$

In this equation, VOI_{CT} and VOI_{PET} denote the volume of interest determined on CT and PET, respectively. In the fourth method, the SUV (both SUV_{max} and SUV_{mean}), metabolic tumor volume, and total lesion glycolysis (TLG) were compared for both PET reconstructions to analyze the effect of spatial matching on quantification of radiotracer uptake.

Statistical Analysis

Since not all the paired groups were normally distributed, statistical analysis was performed using the Wilcoxon signed-ranks test with SPSS Statistics, version 20 (IBM). Statistical significance was defined as a P value of less than 0.05. Data are reported as mean \pm SD.

RESULTS

The average duration of the breath-hold protocol was 12.1 ± 0.91 s. The protocol started with an average of a 4-s interval between the breath-hold instructions and the start of the CT acquisition. This 4-s interval was caused by the standard delay before the CT scan and the observation time that was required to inspect whether the patient was able to comply with the instructions. The CT acquisition itself had an average duration of 8.0 ± 0.55 s, with a scan range of 41.4 ± 3.2 cm.

After practicing the breathing instructions (before the start of the PET/CT scan), all patients indicated that the instructions were feasible. Nevertheless, when patients appeared unable to comply with the instructions during the CT acquisition, they were excluded from analysis, following the method described in the Materials and Methods section. When a cutoff of 0.4 was used for the ratio between the average breathing amplitude before the start of the CT scan and during the CT acquisition, 4 of the 20 patients were excluded. A cutoff of 0.4 was chosen to indicate that on average, the patients could effectively reduce the breathing amplitude by more than half during the end-plateau phase of the respiratory cycle. The average ratio for the group of patients who did comply with the breathing instructions was 0.17 (SD, 0.11; range, 0.04–0.39), whereas the average ratio for the other 4 patients was 0.95 (SD, 0.56; range, 0.59–1.78). Nevertheless, for 2 of these 4 patients, the respiratory signals during the CT scan indicated

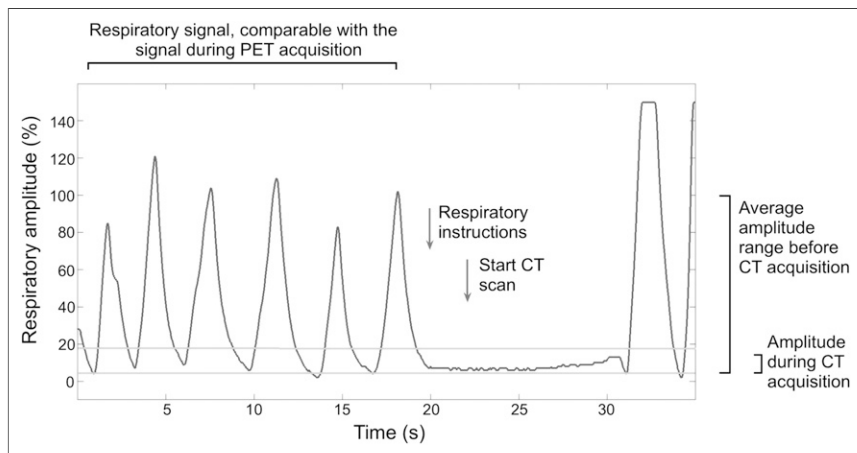


FIGURE 1. Example of respiratory signal before and during CT acquisition. Patients were instructed to hold their breath between amplitude limits of optimal PET gate (between horizontal lines). To determine whether patient complied with instructions, amplitude range of respiratory signal before start of CT scan (mean amplitude range over several respiratory cycles) and during breathing instructions was determined. Ratio between those two was used to determine whether patients were able to hold their breath.

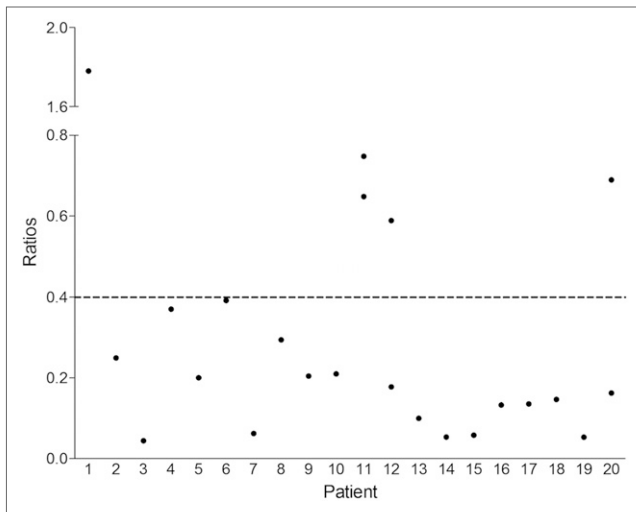


FIGURE 2. Ratios between average amplitude range of respiratory signal during breathing instructions and before CT acquisition, for each patient. Patients 1, 11, 12, and 20 could not comply with breathing instructions and showed higher ratio than other patients. When amplitude during CT acquisition of only lungs (not including upper abdomen region) was considered, ratios of patients 12 and 20 improved; therefore, they could be included in data analysis. Patients 1 and 11 showed only slight or no improvement and were excluded from data analysis.

that they did manage to hold their breath long enough to scan both the lungs and the lung–liver boundary. When the respiratory signal until the acquisition of the lung–liver boundary was considered, the ratio for these 2 patients was lower than the cutoff. Although these 2 patients did not manage to hold their breath during the entire CT acquisition, the area of interest was covered during the breath-hold period and the data were eligible for analysis. The data of the other 2 patients were not included in this study. In Figure 2, the amplitude ratios of the individual patients is shown. For the remaining 18 patients, 17 lung–liver boundaries were determined and 31 lesions were delineated. For one patient, the lung–liver boundary could not be measured on CT because of the presence of pleural effusion.

The results of this study are shown in Table 2, and an example of a patient scan is shown in Figure 3. A significant improvement in the position difference on PET and CT

was detected between the lung–liver boundary when using the breath-hold CT (1.7 ± 2.1 mm), versus the standard CT (5.6 ± 7.3 mm) ($P = 0.049$). For 5 patients, the difference in the lung–liver boundary between PET and standard CT was more than 5 mm, with an average distance of 15.6 ± 5.0 mm. For these 5 patients, the PET in combination with the breath-hold CT showed improved matching in lung–liver boundary, with a mean distance of 1.8 ± 1.6 mm.

The difference in the spatial match of the lesions between gated PET and the standard and breath-hold CT images showed mixed results, even though there was a statistically significant improvement in the distance between the centroids of the lesions between PET and breath-hold CT (3.6 ± 2.0 mm) and between PET and standard CT (5.5 ± 6.5 mm) ($P = 0.040$). There were 9 lesions in the standard CT group with a distance of more than 5 mm. For 8 of these lesions, the difference in centroid location improved when the breath-hold CT was combined with the respiration-gated PET (Fig. 4). However, the Jaccard similarity coefficient showed no significant improvement when breath-hold CT was compared with the standard CT group.

There was a statistically significant difference in radio-tracer uptake when PET images were reconstructed using the standard compared with the breath-hold CT. The average SUV_{mean} increased from 6.1 ± 3.8 mm for the standard CT images to 6.3 ± 3.9 for the breath-hold CT images ($P = 0.044$). SUV_{max} did not show a statistically significant difference between the 2 PET images ($P = 0.104$), nor did the metabolic tumor volume ($P = 0.930$). However, the TLG reached statistical significance, with a slight increment of 0.05 ± 3.37 g for the PET scans reconstructed using the breath-hold compared with the standard CT, with a mean of 54.50 ± 143.4 g and 54.55 ± 143.4 g ($P = 0.018$) for the standard and breath-hold reconstructed PET images, respectively. Although the difference in SUV and TLG were minimal, the breath-hold CT group showed a consistently higher measurement than the standard CT group, resulting in the significant difference between the 2 groups.

The patients included in this study were all suspected of having lung carcinoma, and 8 of these patients also had a diagnosed case of chronic obstructive pulmonary disease (Gold I or II). Two of 4 patients who could not comply with

TABLE 2
Results of Analyses of Spatial Alignment for Both Patient Groups

Parameter	Standard CT and PET	Breath-hold CT and PET	<i>P</i>
Mismatch of lung–liver boundary (mm)	5.6 ± 7.3	1.7 ± 2.1	0.049
Average distance between lesion centroids (mm)	5.5 ± 6.5	3.6 ± 2.0	0.040
Jaccard similarity coefficient	0.32 ± 0.16	0.36 ± 0.16	0.176
SUV_{max} (g/cm ³)	10.3 ± 6.4	10.6 ± 6.6	0.104
SUV_{mean} (g/cm ³)	6.1 ± 3.8	6.3 ± 3.9	0.044
Metabolic tumor volume	6.73 ± 15.6	6.69 ± 15.7	0.930
TLG	54.50 ± 143.4	54.55 ± 141.9	0.018

Data are mean and SD.

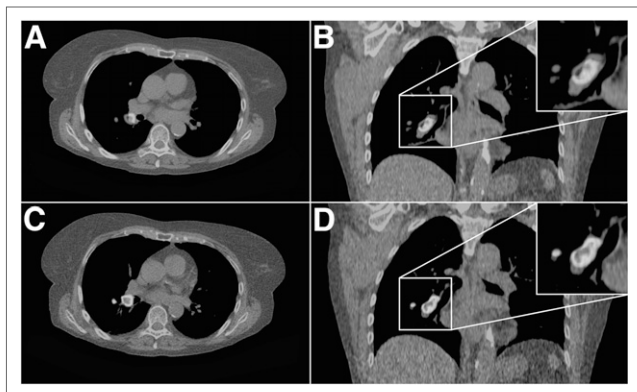


FIGURE 3. Patient with small cell lung cancer. (A and B) Transaxial (A) and coronal (B) planes of standard CT fused with respiration-gated PET image showed mismatch. (C and D) Same transaxial (C) and coronal (D) plane of CT with breathing instructions and corresponding gated PET images showed improved match. (A color version of this figure is available as a supplemental file at <http://tech.snmjournals.org>.)

the breathing instructions had chronic obstructive pulmonary disease. For this study, the patients were instructed to hold their breath for an average of 12.1 s. For the 25 patients, the success rate of the breath-hold procedure was 92% (23/25 patients), indicating that even for this patient cohort the breathing instructions of more than 10 s are feasible.

DISCUSSION

This study shows that spatial alignment between PET and CT images is improved when patient-specific breathing instructions are provided during CT imaging. In this protocol, breathing instructions can be personalized to the individual patient while providing the operator the ability to objectively monitor the performance of the breath-hold maneuver. This study demonstrated improved control over the exact moment to perform the breath-hold maneuver compared with the commonly used end-expiratory breath-hold

method. The technique is relatively easy to implement in clinical practice and results in minimal additional exposure of the patient to ionizing radiation.

However, not all patients could successfully comply with the current breathing protocol, which is an important aspect to consider in this patient population, given that a considerable number of patients have respiratory disorders that can potentially limit compliance. To further improve the proposed method and increase the success rate of the breath-hold, the time for which the breath must be held should be shortened. Optimization of the CT acquisition protocol is a first important step. Scan parameters such as pitch, collimator settings, tube current, and peak voltage can be balanced to acquire CT images with sufficient image quality while reducing scan speed as much as possible. Furthermore, integration of the breathing protocol in the scanner hardware and software can assist in a more efficient initiation and execution of the protocol, preventing unnecessary delays when using external hardware and software, as applied in the current protocol. Furthermore, to appropriately reconstruct the PET images, the CT scan range should match or extend the PET scan range. This can result in unnecessarily long breath-hold CT scans. This PET/CT scanner could acquire PET images only in step-and-shoot mode, for which scanning of an additional bed position required extension of the CT scan range. In several patients, the basal lung fields were positioned outside the second bed position and required the acquisition of a new third entire bed position. In these patients, the scan range of the breath-hold CT needed to be extended, resulting in longer acquisition times. However, several PET/CT scanners on the market are able to acquire data using continuous bed motion. For PET/CT scanners with continuous bed motion, the range of the PET scan can be specifically adapted to the patient's anatomy, without recording an additional full bed position. This capacity can significantly reduce the scan time for the breath-hold CT in these patients (19). Furthermore, in the current protocol, only the PET/CT operator receives feedback on the breath-hold maneuver. An interesting approach would be to provide the patient with either visual or auditory feedback, which can assist the patient in maintaining the required breath-hold amplitude. There are different systems available that can provide this feedback, most of which are already used for radiotherapy applications (20).

Over the years, several strategies have been proposed to reduce spatial mismatching between PET and CT images. Initially, breathing instructions were used during the PET acquisition to create a motion-free image that matched the CT acquisition (2,13). Although these methods have proven useful for reducing the spatial mismatch between PET and CT images, the focus of our respiratory matching protocols has been directed toward modifying the CT acquisition, given that safeguarding the statistical quality of the PET images is important. The advantage is that such approaches optimize the statistical quality of the PET images and the use of the PET data. Although breathing instructions are a

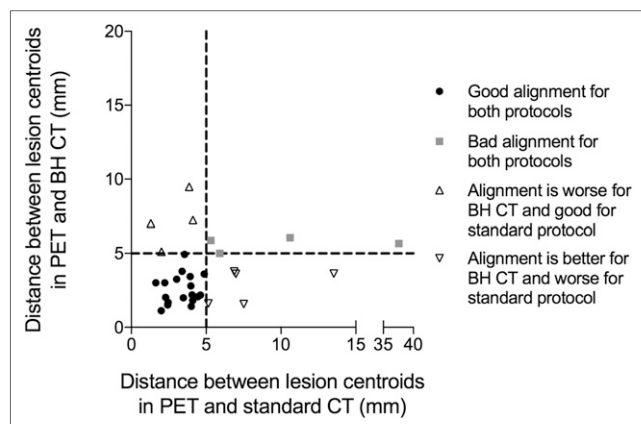


FIGURE 4. Scatterplot showing results of distance between centroids for lesions between PET and breath-hold (BH) CT and between PET and standard CT.

relatively easy way to improve the spatial match between PET and CT images, breathing instructions typically have variable results (8,13,14). This study showed that monitoring the patient's respiration during the breath-hold maneuver reduced this variability and provided a more consistent result regarding the reduction of spatial mismatch between PET and CT.

Besides breathing instructions, several other methods have been proposed to improve the spatial alignment between CT and respiration-gated PET. For instance, various methods that influence the timing of the CT acquisition include respiration-triggered CT (12), in which the (sequential) CT is triggered to the respiration of the patient, or fully gated 4-dimensional CT protocols (1,21), in which a CT image is acquired during all phases of respiration. However, stability in respiratory tracking is still being investigated for the triggered CT approach, and full CT gating is not suitable for routine diagnostics given the high exposure of the patient to ionizing radiation. Other methods include the use of PET list-mode data to elastically transform the PET data to match the CT image (22,23). One of the advantages is that all the PET data can be used for the motion-free PET reconstructions, compared with only 35% of the PET data that were used for the reconstructions made in this study. The last method is increasingly being pursued but still requires validation in larger clinical trials.

The clinical impact of the observed differences in image quantification between PET images would have been relatively modest, with limited effect on SUV, metabolic tumor volume, and TLG. Nevertheless, reducing the effect of spatial mismatch is an important step toward more stable PET quantification. Improving quantitative accuracy is of great importance, since quantitative indices in PET are increasingly being used for therapy response monitoring and radiotherapy planning (11,24). Therefore, improving the reliability and reproducibility of PET image quantification is important. In this study, the maximum difference in SUV between matching and nonmatching PET/CT is 36.5% and 31.5% for SUV_{max} and SUV_{mean} , respectively, indicating that combining optimal respiration-gated PET and breathing-instructed CT can considerably affect SUV quantification.

CONCLUSION

Optimal respiration-gated PET in combination with patient-specific breathing-instructed CT improves alignment between PET and CT images and increases SUV_{mean} and TLG. Even though the effects are small, a more accurate SUV and TLG determination is important for a more stable PET quantification, which is relevant for radiotherapy planning and therapy response monitoring.

DISCLOSURE

During the writing of this article, Charlotte van der Vos received an educational grant from Siemens Healthcare, the

Hague, The Netherlands. No other potential conflict of interest relevant to this article was reported.

REFERENCES

- Nehmeh SA, Erdi YE. Respiratory motion in positron emission tomography/computed tomography: a review. *Semin Nucl Med*. 2008;38:167–176.
- Nehmeh SA, Erdi YE, Meirelles GS, et al. Deep-inspiration breath-hold PET/CT of the thorax. *J Nucl Med*. 2007;48:22–26.
- Goerres GW, Kamel E, Seifert B, et al. Accuracy of image coregistration of pulmonary lesions in patients with non-small cell lung cancer using an integrated PET/CT system. *J Nucl Med*. 2002;43:1469–1475.
- Goerres GW, Burger C, Kamel E, et al. Respiration-induced attenuation artifact at PET/CT: technical considerations. *Radiology*. 2003;226:906–910.
- Van Der Gucht A, Serrano B, Hugonnet F, Paulmier B, Garnier N, Faraggi M. Impact of a new respiratory amplitude-based gating technique in evaluation of upper abdominal PET lesions. *Eur J Radiol*. 2014;83:509–515.
- van der Vos CS, Grootjans W, Osborne DR, et al. Improving the spatial alignment in PET/CT using amplitude-based respiration-gated PET and respiration-triggered CT. *J Nucl Med*. 2015;56:1817–1822.
- Grootjans W, de Geus-Oei LF, Meeuwis AP, et al. Amplitude-based optimal respiratory gating in positron emission tomography in patients with primary lung cancer. *Eur Radiol*. 2014;24:3242–3250.
- Fin L, Daouk J, Morvan J, et al. Initial clinical results for breath-hold CT-based processing of respiratory-gated PET acquisitions. *Eur J Nucl Med Mol Imaging*. 2008;35:1971–1980.
- van Elmpt W, Hamill J, Jones J, De Ruyscher D, Lambin P, Ollers M. Optimal gating compared to 3D and 4D PET reconstruction for characterization of lung tumours. *Eur J Nucl Med Mol Imaging*. 2011;38:843–855.
- Callahan J, Binns D, Dunn L, Kron T. Motion effects on SUV and lesion volume in 3D and 4D PET scanning. *Australas Phys Eng Sci Med*. 2011;34:489–495.
- Boellaard R, Delgado-Bolton R, Oyen WJ, et al. FDG PET/CT: EANM procedure guidelines for tumour imaging: version 2.0. *Eur J Nucl Med Mol Imaging*. 2015;42:328–354.
- Daouk J, Fin L, Bailly P, Meyer ME. Improved attenuation correction via appropriate selection of respiratory-correlated PET data. *Comput Methods Programs Biomed*. 2008;92:90–98.
- Meirelles GS, Erdi YE, Nehmeh SA, et al. Deep-inspiration breath-hold PET/CT: clinical findings with a new technique for detection and characterization of thoracic lesions. *J Nucl Med*. 2007;48:712–719.
- van der Vos CS, Grootjans W, Meeuwis AP, et al. Comparison of a free-breathing CT and an expiratory breath-hold CT with regard to spatial alignment of amplitude-based respiratory-gated PET and CT images. *J Nucl Med Technol*. 2014;42:269–273.
- de Groot EH, Post N, Boellaard R, Wagenaar NR, Willemsen AT, van Dalen JA. Optimized dose regimen for whole-body FDG-PET imaging. *EJNMMI Res*. 2013;3:63.
- FDG-PET/CT accreditation. EARL EANM website. http://earl.eanm.org/cms/website.php?id=/en/projects/fdg_pet_ct_accreditation.htm. Accessed January 30, 2019.
- Erdi YE, Mawlawi O, Larson SM, et al. Segmentation of lung lesion volume by adaptive positron emission tomography image thresholding. *Cancer*. 1997;80:2505–2509.
- Grootjans W, Usmanij EA, Oyen WJG, et al. Performance of automatic image segmentation algorithms for calculating total lesion glycolysis for early response monitoring in non-small cell lung cancer patients during concomitant chemoradiotherapy. *Radiother Oncol*. 2016;119:473–479.
- Acuff SN, Osborne D. Clinical workflow considerations for implementation of continuous-bed-motion PET/CT. *J Nucl Med Technol*. 2016;44:55–58.
- Linthout N, Bral S, van de Vondel I, et al. Treatment delivery time optimization of respiratory gated radiation therapy by application of audio-visual feedback. *Radiother Oncol*. 2009;91:330–335.
- Nehmeh SA, Erdi YE, Pan T, et al. Four-dimensional (4D) PET/CT imaging of the thorax. *Med Phys*. 2004;31:3179–3186.
- Lamare F, Ledesma Carbayo MJ, Cresson T, et al. List-mode-based reconstruction for respiratory motion correction in PET using non-rigid body transformations. *Phys Med Biol*. 2007;52:5187–5204.
- Sun T, Mok GS. Techniques for respiration-induced artifacts reductions in thoracic PET/CT. *Quant Imaging Med Surg*. 2012;2:46–52.
- Grootjans W, de Geus-Oei LF, Troost EG, Visser EP, Oyen WJ, Bussink J. PET in the management of locally advanced and metastatic NSCLC. *Nat Rev Clin Oncol*. 2015;12:395–407.